THE JOURNAL OF BIOLOGICAL CHEMISTRY VOL. 289, NO. 49, pp. 34089–34103, December 5, 2014

A Role for Versican in the Development of Leiomyosarcoma*

Received for publication, September 25, 2014 Published, JBC Papers in Press, October 15, 2014, DOI 10.1074/jbc.M114.607168

Paul A. Keire[‡§], Steven L. Bressler[‡], Joan M. Lemire[§1], Badreddin Edris[¶], Brian P. Rubin[§2], Maziar Rahmani[‖3], Bruce M. McManus[‖**], Matt van de Rijn[¶], and Thomas N. Wight[‡§4]**

*From the [‡]Matrix Biology Program, Benaroya Research Institute at Virginia Mason, Seattle, Washington 98101, [§]Department of Pathology, University of Washington, Seattle, Washington 98195, [¶]Department of Pathology, Stanford University School of Medicine, Stanford, California 94305, and [‖]James Hogg iCAPTURE Centre for Cardiovascular and Pulmonary Research, St. Paul's Hospital, Room 166, 1081 Burrard Street, Vancouver, British Columbia V6Z 1Y6, Canada, and **Department of Pathology and Laboratory Medicine, University of British Columbia, Room G227, 2211 Wesbrook Mall, Vancouver, British Columbia V6T 2A1, Canada*

Background: The cause of leiomyosarcoma (LMS) is unknown.
Results: Experimental modulation of versican levels in LMS cells resulted in altered cell proliferation, adhesion, migration, and tumor growth.
Conclusion: Versican regulates the growth of LMS tumors in a mouse model.
Significance: Collectively, these results suggest targeting versican in the treatment of LMS.

Leiomyosarcoma (LMS) is a mesenchymal cancer that occurs throughout the body. Although LMS is easily recognized histopathologically, the cause of the disease remains unknown. Versican, an extracellular matrix proteoglycan, increases in LMS. Microarray analyses of 80 LMSs and 24 leiomyomas showed a significant elevated expression of versican in human LMS *versus* benign leiomyomas. To explore the importance of versican in this smooth muscle cell tumor, we used versican-directed siRNA to knock down versican expression in a LMS human cell line, SK-LMS-1. Decreased versican expression was accompanied by slower rates of LMS cell proliferation and migration, increased adhesion, and decreased accumulation of the extracellular matrix macromolecule hyaluronan. Addition of purified versican to cells expressing versican siRNA restored cell proliferation to the level of LMS controls, increased the pericellular coat and the retention of hyaluronan, and decreased cell adhesion in a dose-dependent manner. The presence of versican was not only synergistic with hyaluronan in increasing cell proliferation, but the depletion of versican decreased hyaluronan synthase expression and decreased the retention of hyaluronan. When LMS cells stably expressing versican siRNA were injected into nude mice, the resulting tumors displayed significantly less versican and hyaluronan staining, had lower volumes, and had reduced levels of mitosis as compared with controls. Collectively, these results suggest a role for using versican as a point of control in the management and treatment of LMS.

Leiomyosarcoma (LMS)[5] is a mesenchymal form of cancer that originates from smooth muscle cells in dermis or deep soft tissues. LMS can also occur in parenchymal organs, most often the uterus, but is also observed within large blood vessels such as the inferior vena cava. Other than surgical excision, there is presently no cure, and the disease is often fatal if not detected early (1, 2). Although the extracellular matrix (ECM) has been shown to influence the behavior of various tumor types, the role of the ECM in governing the progression of LMS remains uncharacterized.

Versican is an ECM proteoglycan and a member of the large chondroitin sulfate proteoglycan family that interacts with hyaluronan. Versican is known to occur in at least four splice variants: V0, V1, V2, and V3 (3). Versican isoforms V0 and V1 are the predominant isoforms produced by adult smooth muscle cells with V1 as the most abundant form (4). V2 is primarily expressed in neural tissue and not typically by smooth muscle cells, and V3 is variably expressed in a number of tissues but at comparably lower levels than the other isoforms (5). Common to these splice variants are the N- and C-terminal ends, or G1 and G3 globular domains, respectively. The G1 domain of versican, which contains a hyaluronan-binding region, plays a role in mediating cell proliferation, adhesion, and migration, whereas the G3 domain is involved in cell phenotype control

* This work was supported, in whole or in part, by National Institutes of Health Grants HL098067 (to T. N. W.), 5 T32 HG00044 (a training grant through the Stanford Genome Training Program to B. E.), and CA112270 (for work in the van de Rijn laboratory). This work was also supported by American Heart Association Pre-Doctoral Fellowship 0310062Z (to P. A. K.), a National Science Foundation graduate research fellowship (to B. E.), and the National Leiomyosarcoma Foundation and Leiomyosarcoma Direct Research Foundation (for work in the van de Rijn laboratory).
[1] Present address: Dept. of Biology, Tufts University, Medford, MA 02155.
[2] Present address: Dept. of Anatomic Pathology, Cleveland Clinic, Cleveland, OH 44195.
[3] Present address: Genome Sciences Centre, British Columbia Cancer Agency, Vancouver, British Columbia V5Z 4S6, Canada.
[4] To whom correspondence should be addressed: Matrix Biology Program, Benaroya Research Inst. at Virginia Mason, 1201 Ninth Ave., Seattle, WA 98101. Tel.: 206-287-5666; Fax: 206-342-6567; E-mail: twight@benaroyaresearch.org.

[5] The abbreviations used are: LMS, leiomyosarcoma; ECM, extracellular matrix; GAG, glycosaminoglycan; HAS, hyaluronan synthase; LMS/EV, leiomyosarcoma cells transfected with empty vector plasmid; LMS/siRNA Vc, leiomyosarcoma cells transfected with short hairpin sequence specifically targeting versican; LMS/WT, non-transfected wild type leiomyosarcoma cells; LMS/siRNA Scr, leiomyosarcoma cells transfected with siRNA scrambled expression sequence without any known genetically transcribed target.

and cell signaling through its association with integrins, microfibrillar fibulins, and epidermal growth factor (EGF) receptors (for reviews, see Refs. 4 and 6). Between the terminal G1 and G3 domains of versican, are alternatively spliced α- and β-glycosaminoglycan (GAG) attachment domains important to versican biology (7). Versican interacts with hyaluronan, which is a large glycosaminoglycan also shown to be involved in cell migration, adhesion, and proliferation. Hyaluronan is made entirely of repeating disaccharide (D-glucuronic acid β-1,3-*N*-acetylglucosamine-β-1,4) units and is synthesized by three related hyaluronan synthases (HAS1, HAS2, and HAS3).

Molecules such as versican and hyaluronan are present at relatively low levels in normal healthy tissue but then increase dramatically in many different diseases (8–10). Versican and hyaluronan interact to form large macromolecular aggregates around cells that accumulate in a multitude of tumor types (for reviews, see Refs. 6 and 11). The expression of hyaluronan and versican in such a wide variety of cancers suggests an active role for these molecules in tumor development. For example, Sakko *et al.* (12) showed that an increase in versican expression in the ECM facilitates prostate tumor invasion and metastasis by decreasing cell-ECM adhesion. In addition, versican isolated from Lewis lung carcinomas is capable of stimulating inflammatory cytokine production by bone marrow mononuclear cells, thus facilitating metastasis (13). Accordingly, a number of research groups have correlated levels of hyaluronan and versican accumulation with tumor growth and metastatic potential (11, 14–17).

Although a number of studies have shown versican to be up-regulated in various types of cancers and versican levels have been shown to be altered in leiomyoma (18) (the benign neoplastic counterpart to LMS), only a limited number of studies have shown a differential regulation of versican in LMS (19, 20). To further examine the involvement of versican in LMS, we analyzed 12 LMS and three leiomyoma clinical samples by immunohistochemistry and 80 LMSs and 24 leiomyomas by microarray to compare versican expression levels in these malignant *versus* benign neoplasms. Our results indicate that versican protein and mRNA levels are significantly elevated in LMS *versus* leiomyoma. We performed a targeted knockdown of versican using small interfering RNA (siRNA) to examine the role of versican in regulating cell proliferation, migration, cell shape, and substrate adhesion of human LMS cells. The modulation of versican levels exerted a significant influence on tumor cell behavior *in vitro*. Moreover, when injecting nude mice with cells expressing different levels of versican, tumor progression was dramatically altered. Collectively, our results suggest that versican might be an effective target for therapeutic intervention in LMS.

EXPERIMENTAL PROCEDURES

Analysis of Versican Expression and Accumulation in Human LMS Tumor Samples—Tumor samples were obtained from patients with the approval of the University of Washington Institutional Review Board. All tumor specimens were frozen and maintained at −80 °C immediately after resection. Pathologic diagnosis was made by a surgical pathologist (B. P. R.) at the University of Washington Medical Center with experience in the diagnosis of sarcomas according to World Health Organization criteria (21). Histopathologic assignment of whether the tumor was leiomyoma or grade 1, 2, or 3 LMS was determined using the French Federation of Cancer Centers Sarcoma Group grading system, which is based on degree of differentiation, mitotic activity, and necrosis (22).

For immunohistochemistry, a portion of the tumor specimens (from 15 patients with a minimum of three of each tumor grade) was fixed in 10% neutral buffered formalin and then processed into paraffin. Rabbit anti-human versican primary antibody (23) diluted 1:1000 was then applied to the tissue sections, incubated for 2 h at room temperature followed by horseradish peroxidase-labeled goat anti-rabbit secondary, and then developed by standard immunoperoxidase procedures.

For mRNA Northern blot analyses, RNA was isolated from freshly sampled and frozen tissue using TRIzol reagent (Invitrogen) and organic/acidic aqueous phase separation by the methods of Chomczynski (24). Ten micrograms of RNA from each sample was electrophoresed in a 0.8% agarose formaldehyde gel, alkali-denatured (50 mM NaOH, 10 mM NaCl) for improved transfer, transferred to Zetaprobe membrane, and immobilized by UV cross-linking. The blot was then probed with a ^{32}P-labeled cDNA probe specific for human versican and washed as described previously (25). The DNA probe for versican was a 2.4-kb fragment from the β-GAG region encoded on a plasmid kindly provided by Dr. Richard LeBaron (University of Texas at San Antonio).

Tumor Samples, Microarray Preparation, and Gene Expression Analysis—Gene array data for 51 LMS specimens were published previously (26). Data for an additional 29 LMSs and 24 leiomyomas are new to this study. Fresh-frozen tumor samples were obtained as described previously (26). Tissue fragments were homogenized in TRIzol, and total RNA was extracted. Preparation of Cy-3-dUTP-labeled cDNA from reference RNA (Stratagene, Universal human reference RNA, catalog number 740000) and Cy-5-dUTP-labeled cDNA from tumor specimen, microarray hybridization, and washing of arrays were performed as described by Perou *et al.* (27). The microarrays contained ~42,000 cDNA probes representing ~28,000 genes or expressed sequence tags and were printed on polylysine-coated glass slides by the Stanford Functional Genomics Facility. Details of microarray construction were described previously (27). Microarrays were scanned on a GenePix 4000 microarray scanner (Axon Instruments), and fluorescence ratios (tumor/reference; red to green ratio) were calculated using GenePix software. The raw data and the image files are available from the Stanford Microarray Database. Gene expression studies were performed with the approval of the Stanford University Institutional Review Board. Raw data were retrieved and averaged by biosequence IDs. The log(base 2) of the red to green ratio normalized ratio (mean) was retrieved, and spots were filtered by the following criteria: regression correlation, >0.6; Channel 1 mean intensity/median background intensity, >1.5; Channel 2 normalized (mean intensity/median background intensity), >1. A total of 38,585 biosequence IDs had usable spot data that passed the filter criteria. For each sample in the analysis, expression was averaged across all spots corresponding to the versican biosequence ID.

Preparation and Expression of siRNA to Versican in LMS Cells—To determine and select the siRNA that conferred the most effective knockdown of versican, *in vitro* transcribed siRNAs directed at the G1, β-GAG, and G3 regions of versican were used. The siRNA Template Design Tool (Ambion) was used to design the siRNAs, and the National Center for Biotechnology Information Basic Local Alignment Search Tool was used to verify the uniqueness and specificity of the versican target sequences against the human genome. Targeting oligonucleotide template sequences along with complimentary sequences corresponding to the G1 (sequence 1059, 5′-AATTCACCTTCGAGGAGGC-3′), β-GAG (sequence 1361, 5′-AGATTCAGAATCTAAGAAGA-3′; sequence 4592, 5′-AGGATCTGGAGAAGTGGAT-3′), and G3 (sequence 6775, 5′-CTATGGCTGGCACAAATTC-3′) regions were purchased from Sigma-Genosys. A Silencer siRNA construction kit (Ambion) was used to subsequently produce *in vitro* transcribed siRNAs. The annealed and purified siRNA products were quantified spectrophotometrically at 260 nm.

Initially, to test the effectiveness of the siRNAs, 5 or 10 nM concentrations of each siRNA was complexed in GeneEraser (Stratagene) and applied to human SK-LMS-1 (ATCC) cells, which express an abundance of versican (20). This cell line has been useful in a number of studies where researchers examined pharmacological and biological interventions to counteract the high proliferative rate of LMS (28–31). 50,000 LMS cells/well were plated into 6-well dishes and tested in triplicate for each concentration and siRNA target. RNA was extracted 48 h post-transfection using TRIzol. Quantitative real time PCR (Prism7000, Applied Biosystems) was performed to determine the level of versican message for each siRNA *versus* control, which received only nonspecific scrambled sequence and or the transfection reagent.

Derivation of LMS/siRNA Versican (LMS/siRNA Vc), LMS/Empty Vector (LMS/EV) Control, and LMS/siRNA Scrambled (LMS/siRNA Scr) Control Transfection Plasmids—Having determined which siRNA was the most effective at inhibiting versican, two oligonucleotide pairs were synthesized: 1) a 64-mer, 5′-GATCCCAATTCACCTTCGAGGAGGCTTCAAGAGAGCCTCCTCGAAGGTGAATTTTTTTTGGAAA-3′, with its complementary 3′ to 5′ sequence and built-in BamHI and HindIII restriction site overhangs and 2) a scrambled siRNA control, 5′-GATCCACTACCGTTGTTAAGGTGTTCAAGAGACACCTATAACAACGGTAGTTTTTTGGAAA-3′, also with its complementary 3′ to 5′ sequence and built-in BamHI and HindIII restriction site overhangs (both from Sigma-Genosys). These oligo pairs were annealed and then subcloned into a pSilencer-3.1-H1neo (Ambion) plasmid vector containing the H1 RNA *pol III* promoter and neomycin selection cassette. The H1 promoter is well characterized (32) and provides high levels of constitutive expression across a variety of cell types. Multiple clonal isolates of the LMS cell line, SK-LMS-1, originally derived by Fogh and Trempe (33), were used for all the transfection experiments. LMS cells were transfected with pSilencer-3.1-H1-versican-shRNA-neo plasmid vector for versican-directed siRNA production *versus* shScramble and empty vector controls using FuGENE 6 (Roche Applied Science) according to the protocol and selected over 12–14 days using 600 μg/ml neomycin (G418, Invitrogen). The cells were split, and individual cell island clones were selected and isolated and then grown and cultured separately. These cell isolates having been selected now represented only the transfected population of cells and not a heterogeneous population as in the initial *in vitro* transcribed siRNA experiments. Through the course of experimentation, the cells were periodically screened in the presence of selection antibiotics to assure the vector was maintained and still active. RNA from these stable cell lines was isolated using the same RNA extraction protocol, and quantitative reverse transcription-polymerase chain reaction (qRT-PCR) was then performed on siRNA-expressing *versus* empty vector control clones. Assay-on-Demand (Applied Biosystems) primer/probe sets were used to determine mRNA levels of versican. Expression levels were all normalized to either β-actin or TATA-binding protein mRNA.

Analyses of Versican and HASs in LMS Tumor Cells—Versican protein was identified by Western blotting of samples of media from versican siRNA cells and empty vector controls as we have described previously (34). Samples of media were run on a diethylaminoethyl-Sephacel (DEAE) binding column followed by elution using 8 M urea buffer (2 mM EDTA, 3 M NaCl, 50 mM Tris-HCl, 0.5% Triton X-100, pH 7.4) and then ethanol precipitation. The proteoglycans were subjected to chondroitin ABC lyase digestion (3 h at 37 °C) and electrophoresed overnight on a 4–12% gradient SDS-polyacrylamide gel. The resulting bands were transferred to nitrocellulose and blocked with 2% BSA (w/v; Roche Applied Science) in T-TBS (0.1% (v/v) Tween 20, 0.15 M NaCl, 10 mM Tris-HCl, pH 7.4) for 1 h. The nitrocellulose was probed with rabbit anti-human versican polyclonal antibody (23) at a dilution of 1:3000 to detect all versican isoforms followed by three washes with T-TBS. Alkaline phosphatase-conjugated goat anti-rabbit secondary antibody was added (1:20,000 dilution) followed by three washes in T-TBS. Proteins bands were identified using enhanced chemiluminescence CSPD substrate (Tropix) and visualized by fluorography on Kodak XAR-2 film, and the band signal intensity was quantified using NIH ImageJ software.

To analyze the level of mRNA transcripts for versican and HAS1, -2, and -3 in the treated and control cells, total RNA was isolated as described previously (24). Total RNA was quantified by measuring the absorbance at 260 and 280 nm in a Beckman DU640 spectrophotometer. The purity of the samples was always $A_{260}/A_{280} > 1.8$.

Expression of versican and the three hyaluronan synthases (HAS1, -2, and -3) in the treated and the control cells was examined by RT-PCR. Synthesis of single strand cDNA was performed in 50-μl reactions (reagents were purchased from Promega unless stated otherwise) using 1 μg of total RNA, 2 μl of oligo(dT) (Ambion), 2.5 μl of RNase inhibitor (40 units/μl), 5 μl of deoxynucleotide triphosphates (dNTPs), 10 μl of 5× Improm-II buffer, 12 μl of $MgCl_2$ (25 mM), and 2.5 μl of Improm-II reverse transcriptase per RNA sample. Annealing was performed at 25 °C for 5 min, and cDNA single strand synthesis was performed at 42 °C for 90 min. Conditions for RT-PCR amplification were optimized for $MgCl_2$ concentration and temperature using a PTC-200 Peltier thermal cycler (MJ Research, Inc.). PCRs were performed using 1 μl of single

strand cDNA product, 250 μM dNTP, 2 μl of 10× AmpliTaq Gold buffer, 5 pM each primer, 0.75 unit of AmpliTaq Gold enzyme (Applied Biosystems), and $MgCl_2$ (1.6 mM for versican, HAS1, HAS2, and GAPDH and 2.2 mM for HAS3). Versican primers were GCTTTGACCAGTGCGATTACG (forward) and GCACAGCAGTAGACAATTCCG (reverse), HAS1 primers were TTCCTAAGCAGCCTGCGATA (forward) and GGCAGCAGAGGGACGTAGTTA (reverse), HAS2 primers were GCTCGCAACACGTAACGC (forward) and GTGTTTCAGTAAGGCACTTAGATCG (reverse), and HAS3 primers were CCAGATCCTCAACAAGTACGACTC (forward) and CACCACAATGGTTTTTCGG (reverse). PCR cycle conditions were as follows: 10 min of initial enzyme activation at 95 °C, denaturing for 1 min at 95 °C, annealing at 59.5 °C for 1 min, extension at 72 °C for 1 min, and typically 30 cycles for PCR product visualization.

For immunohistochemical visualization of versican in cells, LMS/EV or LMS/siRNA Vc were cultured on 8-well chamber slides for 48 h and immunocytochemically stained using a polyclonal anti-versican antibody (23). Following fixation in 10% formalin and permeabilization in 0.1% Triton X-100, cells were blocked with 10% normal goat serum for 1 h and then incubated with primary rabbit anti-versican antibody overnight (1:1000 in 2% serum PBS). Alexa Fluor 594-labeled goat anti-rabbit IgG (Molecular Probes) was used to visualize primary antibody, and Hoechst 33342 (Molecular Probes) was used to stain nuclei. All images were obtained using a Leica AOBS SP2 confocal microscope and analyzed by Volocity software (PerkinElmer).

Growth, Adhesion, Cell Coat, and Migration Assays of LMS Tumor Cells—Growth, thymidine, and migrations studies were carried out in 6-well plates at 37 °C and 5% CO_2. Equal numbers of cells (50,000) were first plated (24 h) in complete Dulbecco's modified Eagle's medium (DMEM) (0.25 mM glucose, 100 units/ml penicillin, 100 μg/ml streptomycin sulfate, 1 mM sodium pyruvate, 1× non-essential amino acids; Invitrogen) plus 10% fetal bovine serum (FBS). Cells were then fed DMEM without serum and incubated for 72 h. For [^{3}H]thymidine incorporation assays, cell media were changed to DMEM plus 10% FBS. After 9 h, 1 μCi/ml [^{3}H]thymidine was added directly to the culture medium and incubated for an additional 15 h. Incubations were stopped by removing the medium and washing the cells once with ice-cold PBS and then three times with 6% ice-cold trichloroacetic acid (TCA) to precipitate the radiolabeled DNA. Incorporated label was solubilized with 0.1 M NaOH and scraping, and radioactivity was analyzed by liquid scintillation counting (Beckman Coulter model LS-6500). Data were expressed as disintegrations/min (dpm) per cell. For cell counts, cell culture media were changed to DMEM plus 10% FBS after an initial 72 h in DMEM without serum, and cells were harvested at 0, 24, 48, and 96 h and counted using either a Coulter Z1 cell counter or trypan blue and a hemocytometer. Both methods gave comparable values. Differences were noted in plating efficiency when comparing the LMS wild type (LMS/WT), LMS/siRNA Scr, and LMS/EV cells with the versican siRNA LMS cells. The versican siRNA cells adhered strongly but not initially as well even though viability by trypan blue indicated equal numbers of viable cells.

To test the role of purified versican on the adhesiveness, cell coat thickness, hyaluronan retention, and proliferative rate of LMS cells, versican was isolated and purified from bovine aorta using methods described by Hascall *et al.* (35) and Olin *et al.* (36) with modifications. Versican was extracted at 4 °C for 72 h from freshly acquired bovine aorta by first finely grinding the tissue (~440 g wet weight) directly into 4 M guanidine buffer (50 mM NaOAc, 2 mM Na_2EDTA, 10 mM *N*-ethylmaleimide, 25 mM 6-amino-*n*-hexanoic acid, 5 mM benzamidine HCl, 1 mM phenylmethylsulfonyl fluoride (PMSF), pH 5.8) using ~10–15 ml of extraction buffer/g of tissue and then filtered. The extract was dialyzed (12–14-kDa-cutoff dialysis tubing) over five changes (100 liters total) of deionized H_2O. Following dialysis, the sample volume was measured, and solid urea was added to a concentration of 6 M, NaOAc to a final concentration of 0.05 M, NaCl to a final concentration of 0.2 M, along with protease inhibitors. As an initial step to partially purify the proteoglycans, 80 ml of DEAE (Sigma) suspended in 8 M urea buffer (50 mM Tris base, 0.5% Triton X-100, 0.25 M NaCl) were added, mixed for 30 min, and then allowed to settle overnight at 4 °C. The unbound buffer layer was removed, and the DEAE slurry containing the versican was decanted into conical centrifuge tubes. The DEAE was washed in a 4× volume excess of 8 M urea buffer with 0.25 M NaCl five times, spinning down the DEAE between washes. The proteoglycans were eluted using 1 M NaCl urea buffer. The sample was redialyzed through five changes of deionized H_2O, and the product was shell frozen and lyophilized overnight. The sample was then resuspended in 3 ml of 8 M urea buffer (50 mM Tris base, pH 7.0) and run on a Sepharose CL 4B (2 × 85 cm) column pre-equilibrated with 4 M guanidine buffer (50 mM Tris-Base, 0.1% Chaps, pH 7.0) and eluted. For the purposes of identification and determining the purity of versican, chondroitin ABC lyase digestion of the final preparation produced core proteins of ~550 and 500 kDa, corresponding to V0 and V1. The preparation was free of contaminants as judged by Coomassie Blue staining. The two major core protein bands reacted with both versican antibodies tested (2B1 mAb (Seikagaku, Japan) and 12C5 mAb (Developmental Studies Hybridoma Bank, University of Iowa)) and were functional in binding biotinylated hyaluronan prepared as described (37). The highly purified versican was used in native, undigested form for all experiments.

Versican and hyaluronan add-back experiments used equal numbers of cells (50,000) made quiescent in serum-free DMEM for 72 h and then cultured in the presence of complete DMEM and 10% serum ±versican and/or hyaluronan for 40 h. To investigate migration, a monolayer wound repair assay was performed. Cells were grown to confluence in 6-well plates, and then the media were changed to DMEM without serum. Linear wounds were made in the confluent monolayers using a rubber 1-mm stylet (four wounds per well in triplicate). Wounds were imaged at 0, 12, and 24 h using a Nikon Eclipse TE200 inverted microscope equipped with a Nikon Coolpix E995. Wound areas were determined using ImagePro Plus (Media Cybernetics) and expressed as a percentage of the area at time 0, which was taken as 100%.

Hyaluronan Enzyme-linked Sorbent Assay—To determine whether the levels of hyaluronan were altered in the tumor cells

in which versican production had been decreased, hyaluronan levels were measured by a competitive enzyme-linked sorbent assay modified from that described previously (38, 39). Normal myometrium smooth muscle cells (Cambrex) and LMS/WT cells (SK-LMS-1) were compared with multiple LMS/siRNA Vc clones. Briefly, media from 3-day cultures were harvested and then digested with Pronase (500 μg/ml) in 0.5 M Tris base, pH 6.5 overnight at 37 °C. Following digestion, the Pronase was inactivated by heating to 100 °C for 20 min. The samples were mixed with biotinylated proteoglycan (38) and then added to a hyaluronan-coated microtiter plate and incubated for 1 h at room temperature. Plates were washed, and 100 μl of streptavidin-labeled peroxidase (2 μg/ml) was added to each well and incubated for 30 min at room temperature. Plates were washed, and then 100 μl of 2,2′-azino-bis(3-ethylbenzothiazoline-6-sulfonic acid) in 0.1 M sodium citrate, pH 4.2 was added. The resulting absorbances were measured at 405/570 nm on an OPTImax microplate reader (Molecular Devices) using SOFTmax PRO (version 4.3) software (Molecular Devices). Readings at 570 nm were subtracted from those at 405 nm to account for plate imperfections. The final signal was inversely proportional to the level of hyaluronan in the medium.

Role for Versican in LMS Pericellular Coat Size—The pericellular matrix morphometric analysis was performed as described previously (40). Briefly, 100,000 cells were plated in 6-well tissue culture plates in DMEM containing 10% FBS. On the following day, the cells were made quiescent in low serum for 48 h and then cultured in the presence or absence of versican. After 24 h, 600 μl of a suspension of fixed and washed human erythrocytes ($\sim 10^8$/ml) was added to the cells and allowed to settle for 15 min. Pericellular matrix formation was quantified using images captured on a Leica inverted microscope equipped with an Insight model 14.2 Color Mosaic camera (Diagnostic Instruments). The Advanced Spot (Diagnostics Instruments) Windows version 4.6 acquisition software allowed precise measurements of the coat thickness defined as the matrix excluding the erythrocytes perpendicular to the cell body.

Hyaluronan Processing by the LMS Tumor Cells—To determine the role of versican in hyaluronan processing, cells were cultured for 24 h in the presence of 10% FBS. At 24 h, the media were changed to 10% complete DMEM with or without FITC-labeled hyaluronan. At 72 h, the cells were trypsinized, replated at 100,000 cells/well, and cultured an additional 24 h in the presence or absence of versican. The level of fluorescence indicated the level of hyaluronan processing and retention by the cell. Images were acquired using a Leica DM2500 microscope with Leica N Plan objectives and an Insight model 14.2 Color Mosaic camera. The acquisition software was Advanced Spot Windows version 4.6, and NIH ImageJ software was used to threshold the image data (count pixels) to determine the level of hyaluronan processing.

Analyses of Tumor Growth in the LMS Nude Mouse Tumor Model—A well established tumor cell growth model (31) was used combined with the clonal populations of the human uterine tumor cell line SK-LMS-1 described above. A total of 30 mice were treated. Twelve immunocompromised BALB/c nude mice (Charles River Laboratories) each received 2×10^6 LMS/siRNA Vc knockdown cells on one dorsal flank subcutaneously, six received 2×10^6 LMS/siRNA Scr cells, six received 2×10^6 LMS/EV cells, and six received 2×10^6 LMS/WT cells. The mice were observed every day after the initial injection, and tumor volumes were measured (see below) from the living animals. At the end of the study, the animals were euthanized, and the tumors were excised for further histological analyses to determine versican and hyaluronan expression levels and tumor mitotic index. This study was approved by the Benaroya Research Institute Animal Care and Use Committee, and care and use of the experimental animals were carried out in accordance with the United States Animal Welfare Act.

The volume of the tumor (V) was determined on the basis of three mutually orthogonal measurements (X, Y, and Z) of the tumor nodule made using a high precision (accurate to 0.001 mm) digital caliper. As in a previous report, the formula $V = XYZ\pi/6$ was used to calculate tumor volume (41). The number of tumors used for volume measurements in each group was as follows: LMS/siRNA Vc, 11; LMS/siRNA Scr, 6; LMS/WT, 6; and LMS/EV, 5.

After 21 days of tumor growth, the mice were sacrificed. The tumors were excised, fixed in 10% neutral buffered formalin for 24 h, and then processed into paraffin. Five-micrometer sections were used for hematoxylin and eosin (H&E) staining and all histochemical and immunofluorescence staining. Mitotic figures were counted in 10 randomly selected high power fields (400×) per section and expressed as a mitotic index. Mitotic figures were counted in five sections from each tumor (LMS/EV control *versus* LMS/siRNA Vc), and mitotic index values were compared. Three LMS control tumors and three versican siRNA LMS tumors were used for histologic evaluation and mitotic counting.

Statistical Analysis—Student's t test was used to determine statistical significance of all analyses except in the microarray analysis where a Fisher's exact test was also used. These statistical analyses were performed using Microsoft Excel version 14.0. Differences were considered significant when p was <0.05.

RESULTS

LMS Tumors Accumulate Versican—Tissue samples taken from 15 patients were identified as either benign leiomyoma or one of three grades of smooth muscle cell tumor (LMS grades 1–3), and four patients with normal myometria were used as controls. Normal myometrial controls displayed limited if any versican immunostaining (Fig. 1*A*), and the leiomyoma samples displayed slightly more versican staining (Fig. 1*B*), whereas all the LMS tumor grades (Fig. 1, *C–E*) indicated intense and widely distributed versican staining. The staining pattern for versican in the tumor samples in terms of intensity and distribution was consistent for all the samples tested. Histologically, the malignant tumors grew in interlacing bundles of smooth muscle cells displaying multifocal, moderate to severe cytologic atypia and a mitotic index of greater than 10 mitotic figures per 10 high power fields for higher grade tumors. Tumor grades 1 and 2 showed the most intense versican staining, and areas of high versican accumulation corresponded to areas of the greatest cellularity in the lower grade tumors. Northern blot data

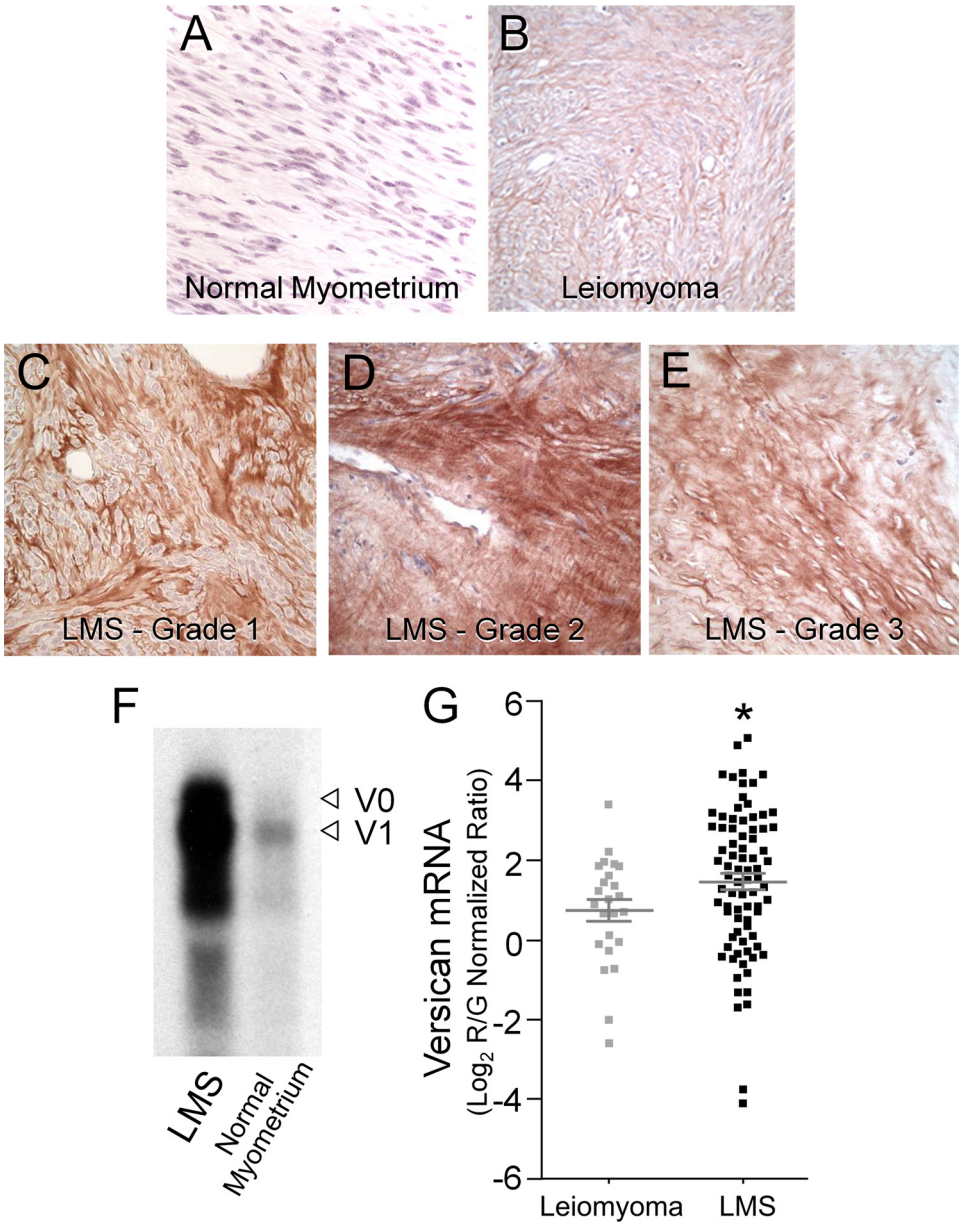

FIGURE 1. **Versican is highly expressed in clinical samples of leiomyosarcoma tissue.** Histological assessment of normal myometrium shows low to undetectable levels of versican expression (*A*) and an increase in versican levels in leiomyomas (*B*) when compared with normal myometrium. This increase, however, is intermediate and less than that found in grade 1, 2, and 3 leiomyosarcoma tumors. The three grades of tumor (LMS grades 1–3; *C–E*) express comparably more versican. Grade 1 and grade 2 LMS tumors (*C* and *D*) displayed the greatest versican expression in terms of both intensity and distribution. The increased cellularity in lower grade tumors appeared to correspond to areas of high versican expression. *Original magnification*, 400×. *F*, Northern blot analyses of LMS tissue show a high level of versican transcript *versus* adjacent normal myometrial controls. The blot represents loading based on equal amounts of 28 S RNA. *Arrowheads* (◁) indicate versican isoform bands V0 and V1 on the basis of size, *top* to *bottom* (79). *G*, versican mRNA is up-regulated in LMS *versus* benign leiomyoma. Scatter plots are shown for versican mRNA expression levels in clinical samples of 80 LMSs and 24 benign leiomyomas as analyzed by gene expression microarrays. On average, LMS samples showed an approximate 2-fold increase in versican transcript levels when compared with leiomyoma samples, which represented a statistically significant up-regulation, *R/G*, red-to-green ratio (mean ± S.E. (*error bars*); *t* test, *, $p = 0.0365$).

from homogenized LMS tumors indicated significantly higher versican mRNA levels *versus* adjacent normal myometrium (Fig. 1*F*).

To further understand whether versican plays a tumor-promoting role in soft tissue neoplasms, we analyzed gene microarray expression data from 80 LMSs and 24 leiomyomas (Fig. 1*G*). On average, versican mRNA showed a 2-fold up-regulation in expression in LMS samples *versus* leiomyoma, which represented a statistically significant increase (*t* test, $p = 0.0365$). Furthermore, when ranking all 104 cases by versican mRNA level and adjusting for the relative number of each sample type, cases with higher than average versican expression levels were significantly more likely than cases with lower than average versican expression levels to be LMS (Fisher's exact test, $p = 0.0026$). Together, these results are consistent with the notion that versican may play a role in mediating the aggressiveness of LMS tumors as compared with benign leiomyomas.

Versican-directed siRNA—LMS cells were treated with individual *in vitro* transcribed siRNAs specifically directed and spaced along the length of versican mRNA. Quantitative RT-

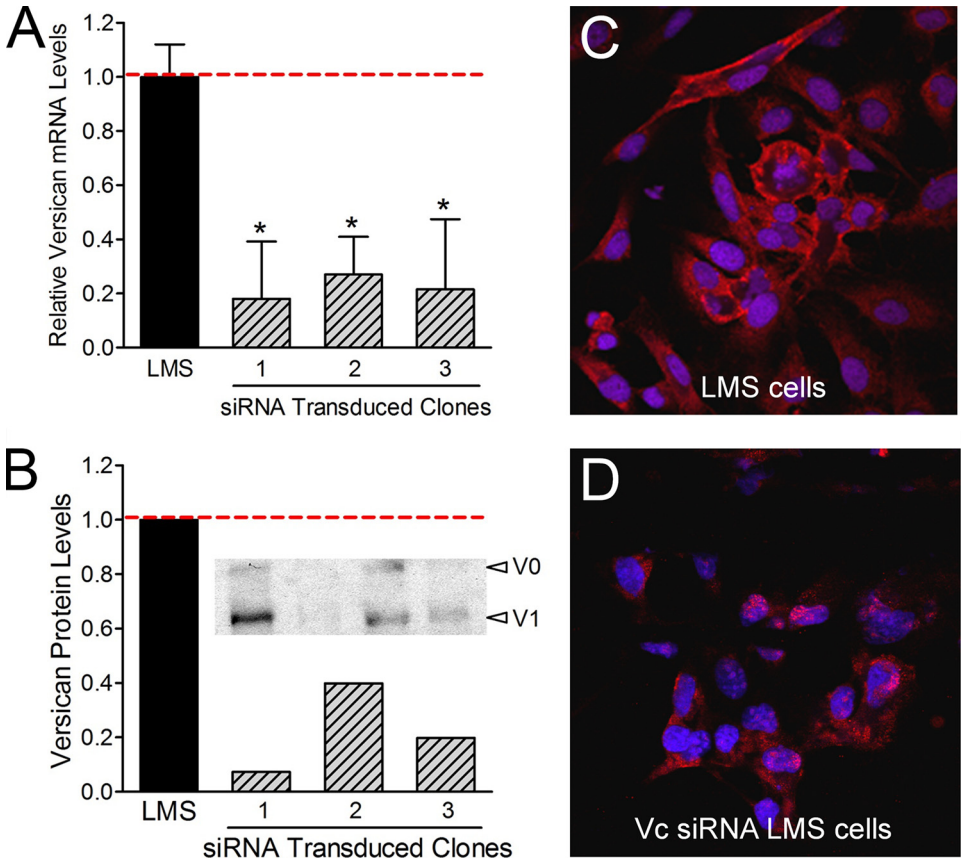

FIGURE 2. **Versican siRNA efficiently inhibits versican expression.** By constitutive expression of versican siRNA in LMS cells, as much as an 85% reduction in versican mRNA (*A*) and a 95% reduction in versican protein were achieved (*B*). * represents statistical significance ($p < 0.05$) between LMS/siRNA Vc clones (*1*, *2*, and *3*) compared with LMS control cells (*error bars* represent ±S.D.). Densitometry of the Western blot (*B*) depicts the relative versican protein levels for the V1 isoform. *C* and *D*, LMS/EV or LMS/siRNA Vc cells were cultured for 24 h on 8-well chamber glass slides. Cells were fixed and immunocytochemically stained for versican (*red*). Cell nuclei were counterstained with Hoechst 33342 (*blue*). Immunocytochemical analysis confirmed that versican levels were significantly reduced in the LMS/siRNA Vc cells.

PCR mRNA analyses revealed that the 5′-G1 domain-directed siRNA (1059) was the most effective at inhibiting versican (55 ± 1.8% reduction *versus* 18 ± 3.2% for the 1361, β-GAG domain-directed; 10 ± 2.1% for the 4592, β-GAG domain-directed; and 22 ± 3.7% for the 6775, G3 domain-directed siRNAs). Subsequently, the corresponding 1059 siRNA cDNA was successfully subcloned into the pSilencer-3.1-H1neo plasmid expression vector with its neomycin selection cassette. The proper orientation and sequence of the insert were confirmed by nucleotide sequencing. Thus, when transfected into LMS cells, stable clones with constitutively reduced versican levels were successfully produced.

When measured by quantitative RT-PCR, an 85% reduction in versican mRNA was achieved (Fig. 2*A*), and a 95% reduction of versican protein levels was detected by Western blot (Fig. 2*B*). These results were supported by immunofluorescence analysis that showed a significant decrease in versican staining associated with the cells as compared with the LMS empty vector control cells, which produced abundant versican (Fig. 2, *C* and *D*).

Reducing Versican Expression by siRNA Alters LMS Tumor Cell Shape and Adhesion—Morphologically, the LMS/WT, LMS/EV, and LMS/siRNA Scr control cells were spindle-shaped and spread rapidly (Fig. 3*A*), whereas the LMS/siRNA Vc cells were flatter, more polygonal, and grew in tight rounded islands (Fig. 3*B*). In addition, the trypsinization time for complete cell removal from cell culture plastic changed with changing versican levels. The time for cells to be removed from cell culture plastic was ~10 times longer for the LMS/siRNA Vc cells *versus* the LMS/WT, LMS/EV, or LMS/siRNA Scr control cells (Fig. 3*C*). Addition of versican to the LMS/siRNA Vc cells reversed the adhesive phenotype as evidenced by the reduction of trypsinization time for removal of the LMS/siRNA Vc tumor cells from the culture dish with added versican (Fig. 3*C*).

Reducing Versican Expression by siRNA Decreases LMS Tumor Cell Proliferation and Migration—The LMS/siRNA Vc cells in which the versican had been reduced by versican-directed siRNA had significantly decreased proliferation and migration rates (Fig. 4). Furthermore, the incorporation of [^{3}H]thymidine into DNA was significantly reduced in versican siRNA-transfected cells when compared with LMS/EV and LMS/siRNA Scr controls (Fig. 4*A*). This was observed for all the LMS/siRNA Vc cell clones tested ($n = 7$). The increase in cell number over time was also significantly reduced for the LMS/siRNA Vc cells (Fig. 4*B*). However, this reduction of LMS tumor cell growth by reducing versican levels could be reversed if versican was added back to the LMS/siRNA Vc cell cultures in a dose-dependent manner (Fig. 4*C*). To evaluate the impact of reducing versican on LMS tumor cell migration, a scratch wound assay was performed using confluent LMS cells.

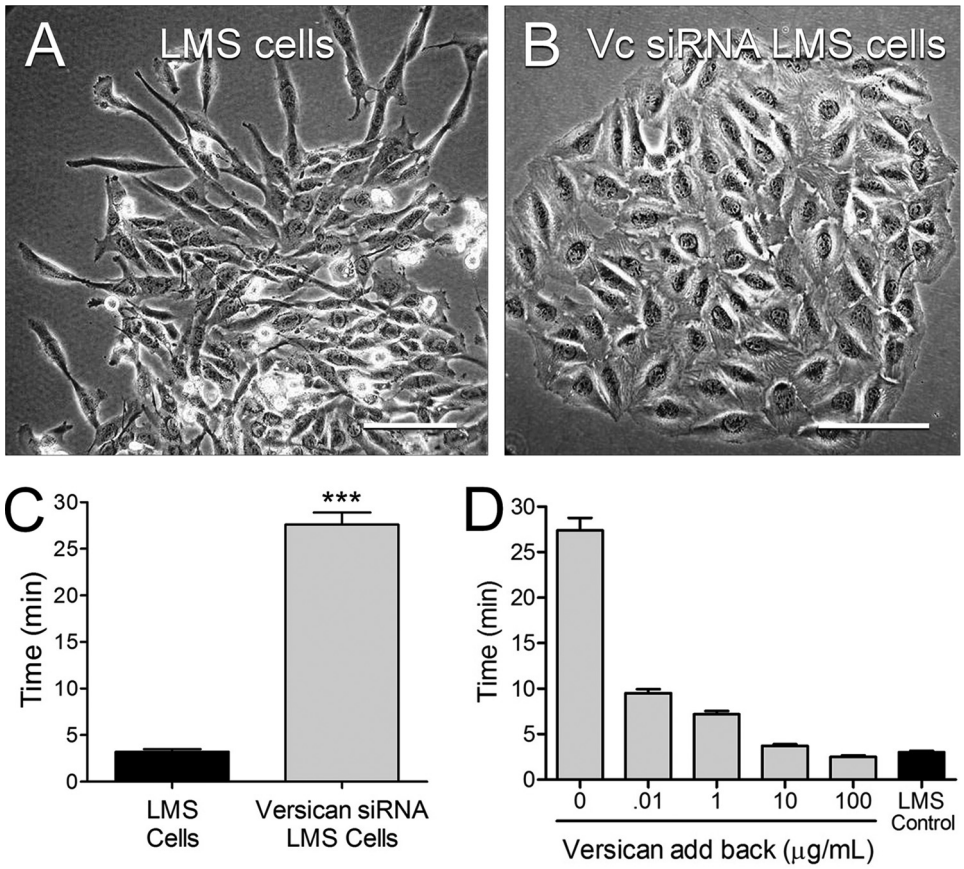

FIGURE 3. **LMS/siRNA Vc cells are more polygonal, have a less migratory phenotype, and are more adhesive to cell culture plastic compared with LMS cells.** *A*, LMS/EV (shown), LMS/WT, and LMS/siRNA Scr control cells growing from clonal islands assume spindle shapes typical of rapidly proliferating smooth muscle cells. *B*, in contrast, LMS cells transduced to express versican siRNA are flatter, more polygonal, and cluster into aggregates. *Scale bars*, 30 μm. *C*, trypsinization time for complete removal of the cells was ~10 times longer for the versican siRNA cells (*gray bar*) than the LMS/EV controls (*black bar*) ($n = 6$) (***, $p < 0.0001$). *D*, addition of versican to the LMS/siRNA Vc cells reversed the adhesive phenotype in a dose-dependent manner. *Error bars* represent ±S.E.

LMS/siRNA Vc-treated cells migrated at a significantly slower rate than LMS/WT control cells (Fig. 4*D*).

Reducing Versican Expression by siRNA Reduces LMS Tumor Cell Production of Hyaluronan and Pericellular Coat Formation—Because the medium from LMS tumor cells was highly viscous with a gel-like consistency and the medium from the LMS/siRNA Vc-modified cells was not, we examined the media for the presence of hyaluronan. Strikingly, the LMS/siRNA Vc clones produced significantly less hyaluronan closer to normal myometrial cell production levels compared with the LMS cells, which produced much more hyaluronan (Fig. 5*A*). Moreover, HAS2 and HAS3 expression in the LMS/siRNA Vc clones was 3–4-fold less than LMS controls (Fig. 5*B*). HAS1 was not detected in either LMS tumor cells or LMS/siRNA Vc-modified cells (data not shown). These results indicate that hyaluronan synthesis and/or accumulation by LMS tumor cells is in some way linked to the synthesis of versican by these cells.

To determine the contribution of hyaluronan and versican to LMS tumor cell proliferation, hyaluronan and versican were added separately or together to LMS/siRNA Vc cells. The addition of exogenous, high molecular weight hyaluronan led to a significant 20% increase in cell number for the LMS/siRNA Vc cells ($p = 0.015$); however, the effect with the addition of exogenous versican was significantly greater ($p = 0.0006$), leading to a 270% increase in the number of LMS/siRNA Vc cells and near complete restoration to LMS/EV control tumor cell numbers (Fig. 5*C*). Moreover, an additive or synergistic effect between hyaluronan and versican was observed as the increase in cell number by versican alone was lower in comparison with the combination of hyaluronan and versican together ($p = 0.004$).

Because both hyaluronan and versican contribute to pericellular coat formation during the proliferative and migratory phases of several cell types (for a review, see Ref. 42), we asked whether differences existed in the extent of pericellular coat formation between LMS tumor cells and LMS tumor cells in which versican and hyaluronan had been reduced by siRNA to versican. Using a particle exclusion assay, the presence of a distinct pericellular matrix around cultured cells was demonstrated by the exclusion of fixed red blood cells. LMS tumor cells exhibited an extensive pericellular coat (Fig. 6, *A* and *D*), whereas this coat was significantly reduced in the LMS/siRNA Vc cells (Fig. 6, *B* and *D*). However, adding exogenous versican to LMS/siRNA Vc cells restored the thickness of the pericellular coat in a dose-dependent manner (Fig. 6, *C* and *D*). We also added back versican and hyaluronan to the control transfected LMS cells and found little if any additional increase in cell proliferation or cell coat thickness (no significant increase was observed; data not shown). We next tested what role versican was playing in the maintenance, processing, and/or retention of

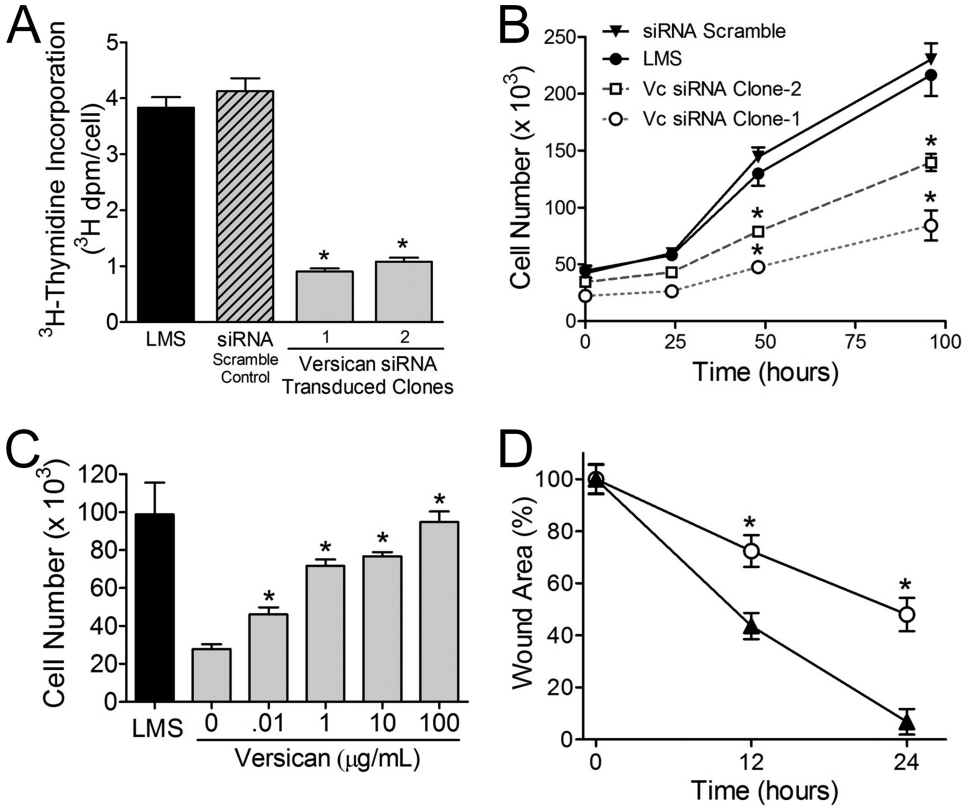

FIGURE 4. **DNA replication, cell proliferation, and migration are inhibited by versican knockdown; however, cell proliferation is reversible by versican add-back.** [^{3}H]Thymidine levels (*A*) and cell proliferation (*B*) indicate that the LMS/WT (●) and LMS/siRNA Scr (▼) control cells divide and proliferate at a significantly higher rate than the two different versican siRNA LMS cells (□ and ○). *C*, the reduction in the proliferative rate induced by versican siRNA can be reversed by the addition of purified versican to the culture medium. Exogenous versican exerts its effect in a dose-dependent manner (*, $p < 0.05$; analyzed at 40 h). *D*, in a wound migration assay, the migration of LMS cells (▲) was significantly greater (*, $p < 0.05$) at 12 and 24 h than that of LMS cells transduced with versican siRNA (○) ($n = 4$). *Error bars* represent ±S.E.

hyaluronan by providing FITC-labeled hyaluronan for 72 h to versican-depleted LMS/siRNA Vc cells and then replating the cells in the presence or absence of versican. The cells that were supplemented with purified exogenous versican maintained the FITC-labeled hyaluronan to a significantly greater extent (Fig. 6, compare *E*–*G*), indicating that versican increased the retention and/or decreased the degradation of hyaluronan.

Tumor Induction in Nude Mice—To test the impact of versican synthesis on tumor development, either LMS/WT, LMS/EV, or LMS/siRNA Scr controls or LMS cells constitutively expressing versican siRNA were injected into nude mice, and tumor growth was examined over a 3-week period. H&E staining of the LMS/WT, LMS/EV (shown), and LMS/siRNA Scr tumor control groups revealed tumor cells separated by ECM, whereas the LMS/siRNA Vc tumors contained cells that were smaller and separated by less ECM (Fig. 7, *A* and *B*). Immunohistochemical analysis of versican and hyaluronan revealed that the empty vector control LMS tumors continued to accumulate high levels of versican and hyaluronan (Fig. 7, *C* and *E*), whereas the versican siRNA LMS tumors were smaller and had very low levels of versican and hyaluronan (Fig. 7, *D* and *F*).

Analysis of tumor volume demonstrated a marked reduction in tumor growth in animals injected with LMS/siRNA Vc cells (Fig. 7*G*). A linear mixed model was fit to the data in Fig. 7*G* with time, group, and time × group as fixed effects and mouse as a random effect. The model showed that the differences in the tumor volume changes over time were statistically significant between the three groups ($p < 0.0001$) with the LMS/siRNA Scr and LMS/EV experimental groups showing the greatest increases over time and the LMS/siRNA Vc showing the smallest increase over time. In support of these findings, mitotic index analyses were 3–4-fold lower for the LMS/siRNA Vc cells compared with the LMS/EV cells (Fig. 7*H*).

DISCUSSION

The results of this study indicate that versican expression and content are elevated in human LMS tumors when compared with normal myometrium and benign leiomyomas. Increased versican levels have been observed in breast and prostate cancers (20, 43) and are associated with high metastatic potential and poor prognosis in patients with cervical (44), laryngeal (45), testicular (14), and gastric (46) cancers but have not been fully characterized in LMS. In contrast to these epithelial carcinomas, LMS tumors are derived from smooth muscle cells of mesothelial origin in the stroma of the affected organ. Moreover, in all of these tumor types, including LMS, versican expression levels are positively correlated with tumor grade, indicating a poor prognosis. What is not clear, however, is how high levels of versican impact tumorigenesis.

Versican in LMS and the Regulation of Tumor Cell Phenotype—The results of our study detail and link the ability of the LMS tumor cells to synthesize versican and their ability to

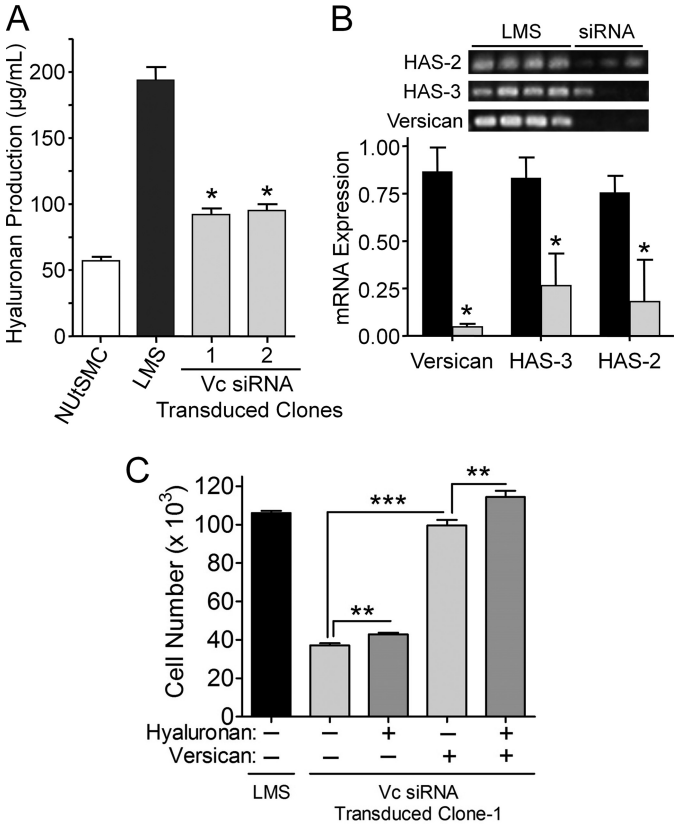

FIGURE 5. **Reduction in hyaluronan and HAS levels with a reduction in versican synthesis.** *A*, a decrease in hyaluronan production levels followed versican levels knocked down by siRNA. LMS/siRNA Vc clones (*gray bars*) along with normal uterine smooth muscle cell (*NUtSMC*) controls (*open bar*) produce significantly less total hyaluronan than the LMS/WT tumor cells (*black bar*) and on an equal cell basis (*, $p < 0.05$). *B*, RT-PCR for HAS2, HAS3, and versican for LMS/WT control tumor cells and LMS/siRNA Vc cells (*upper panel*) in which versican mRNA had been constitutively reduced using versican-directed siRNA. Densitometry of RT-PCR averaged control ($n = 4$) (*black bars*) or siRNA clones ($n = 3$) (*gray bars*) showed a significant reduction in the levels of HAS2, HAS3, and versican in the cells expressing versican siRNA (*, $p < 0.05$). All lanes were normalized to GAPDH. *C*, large molecular weight hyaluronan by itself does not restore the proliferative profile of LMS/siRNA Vc cells to LMS/WT levels but does with the addition of purified versican. Although there is a significant increase in cell proliferation with the addition of hyaluronan (30 μg/ml; *, $p < 0.015$), the increase due to the addition of versican at nanogram levels is significantly greater (***, $p < 0.0001$), and near complete restoration (96.6%) of the cell native proliferative rate is achieved at 100 μg/ml versican. The difference between versican alone and versican + large hyaluronan is significant (**, $p < 0.004$), suggesting an additive or synergistic effect between hyaluronan and versican on cell proliferation. *Error bars* represent ±S.D.

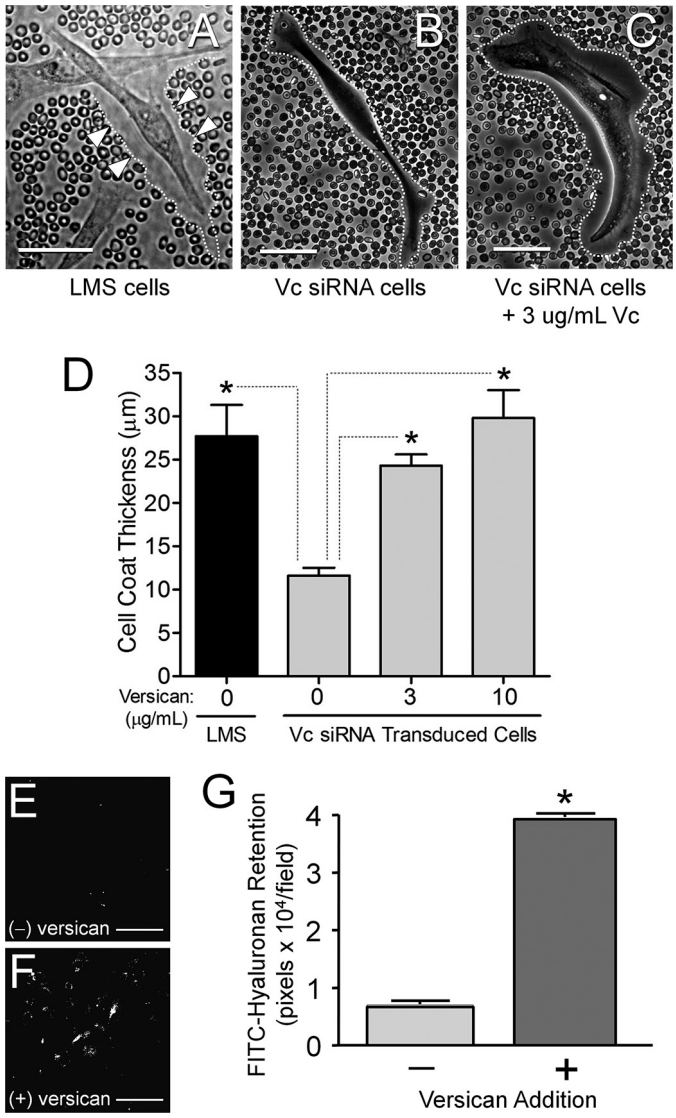

FIGURE 6. **Versican increases pericellular coat thickness and limits hyaluronan degradation.** *A*, LMS/WT (shown), LMS/EV, and LMS/siRNA Scr control cells have prominent pericellular coats. *Arrowheads* (▷) and *dotted white lines* mark the pericellular boundaries. *B*, LMS/siRNA Vc cells display a diminished cell coat, which increases in thickness with the addition of exogenous versican (*C*). Individual cells were examined with a particle exclusion assay 24 h after the addition of versican. Measurements were perpendicular to the cell membrane at the point of maximum coat thickness. *Scale bars*, 50 μm. The cell coat thickness of the LMS cells is significantly greater than the LMS/siRNA Vc cells (*, $p < 0.05$) and increased significantly (*, $p < 0.05$) with the addition of exogenous versican to the cell medium. *D*, bar graph representing the average ± S.E. of $n = 172$ cells counted for control LMS cells, $n = 293$ LMS/siRNA Vc cells with 0 μg/ml versican, $n = 104$ cells with 3 μg/ml versican, and $n = 67$ cells with 10 μg/ml versican. *E–G*, degradation of internalized FITC-hyaluronan is inhibited in the presence of versican. Media for versican-depleted LMS/siRNA Vc cells was supplemented with FITC-labeled hyaluronan for 72 h, and then the cells were trypsinized and replated. After 24 h, the amount of FITC-labeled hyaluronan was measured in the absence (*E*) or presence (*F*) of 10 μg/ml purified versican. *Scale bars*, 100 μm. Cells receiving versican retained a significantly greater amount of hyaluronan (*, $p < 0.001$) (*G*). *Error bars* represent ±S.D.

migrate, proliferate, adhere, and synthesize ECM hyaluronan. Such findings implicate versican as an ECM molecule capable of regulating several aspects of LMS tumor cell phenotype. Furthermore, knocking down versican expression in LMS tumor cells had a dramatic effect on tumor growth in an LMS mouse model, confirming a critical role for this ECM macromolecule in LMS tumor progression.

Tumorigenesis is a multistage process involving aberrant proliferation, tissue invasion, destruction of adjacent tissue, and metastatic growth or spread to other locations in the body. These malignant properties of cancers differentiate them from benign tumors, which are self-limited in their growth and with rare exception do not invade or metastasize. Although versican is known to accumulate in benign neoplasms of leiomyoma (18), we found that mRNA levels for versican were significantly greater in leiomyosarcomas *versus* leiomyomas, suggesting that versican may have a role in the invasiveness of the malignant LMS tumors. Along these lines, Mäkinen *et al.* (47) showed that mutations in MED12, a mediator complex subunit gene located on the X chromosome, are found in 70% of benign leiomyomas.

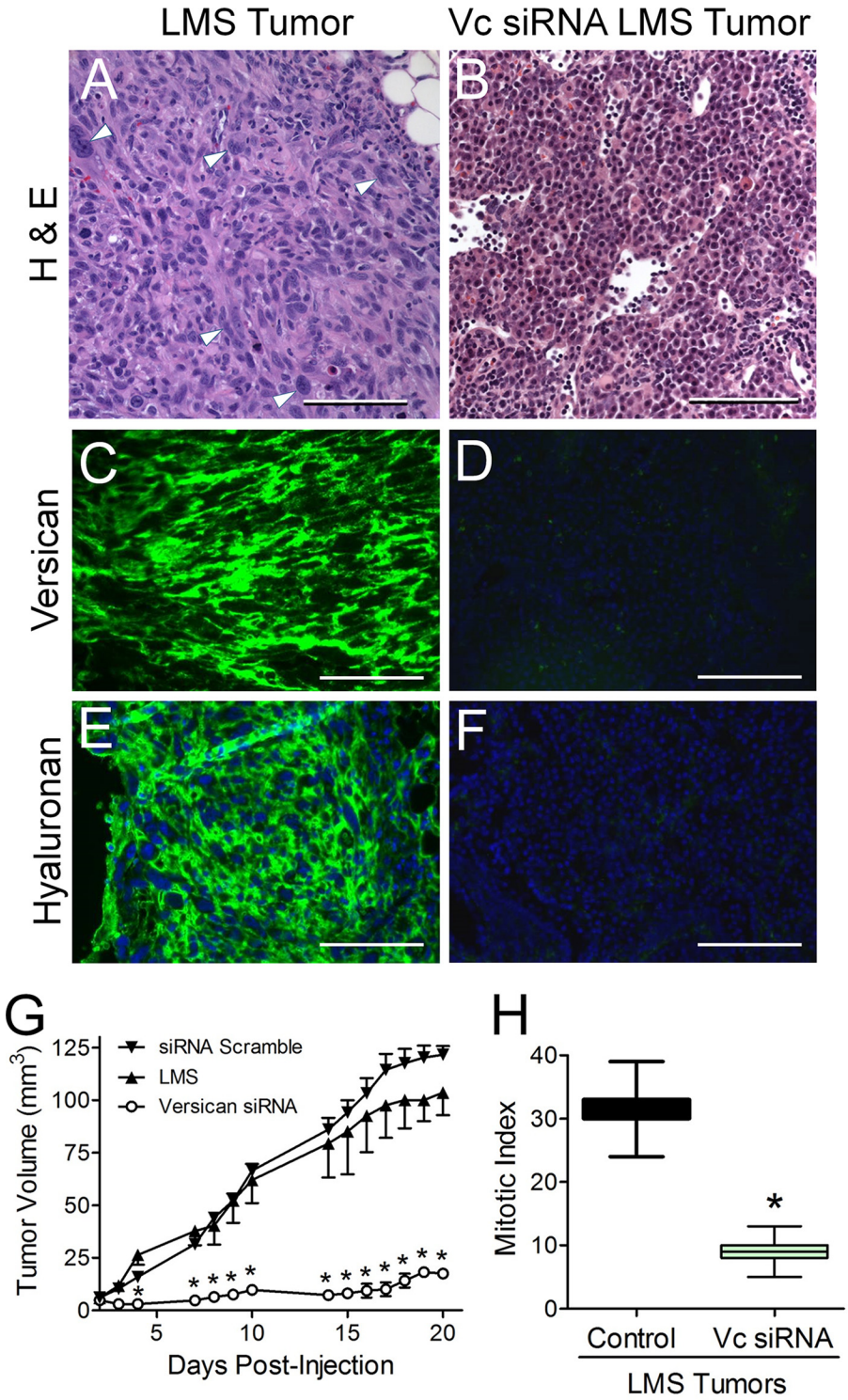

FIGURE 7. **Versican and hyaluronan are highly expressed in LMS tumors in comparison with versican siRNA tumors.** LMS tumors also grow continuously with a high mitotic index, whereas versican siRNA tumors grow only slowly and at one-third the mitotic index. Images (*A–F*) represent subcutaneous tumors excised after 21 days in nude mice; all image pairs were taken at equal exposure. H&E staining of tumor sections reflects a highly hyperplastic cellular response in the LMS tumors (*A*) not seen in the versican siRNA tumors (*B*). Multinucleation, cytologic pleomorphisms (*arrowheads*), and tissue necrosis were observed in LMS tumors, whereas less cellular atypia and no evidence of necrosis were observed in the versican siRNA tumors. *Scale bars*, 100 μm. *Original magnification*, 400×. The constitutively expressing versican siRNA LMS cells (panels on the *right*) only faintly express versican (*D*) and hyaluronan (*F*) compared with the tumors of the empty vector control panels on the *left* (*C*, versican; *E*, hyaluronan). Over the 3-week study period, the LMS tumors grew continuously (*G*) with a high mitotic index (*H*), whereas versican siRNA tumors grew slowly and at one-third the mitotic index. *G*, tumor volume over time in nude mice injected subcutaneously in LMS/EV (▲; $n = 5$; ±S.E.) and LMS/siRNA Scr (▼; $n = 5$; ±S.E.) control cell tumors *versus* LMS/siRNA Vc cell tumors (○; $n = 11$; ±S.E.). *, $p < 0.001$. *Error bars*, ±S.E. *H*, mitotic index of LMS control cell tumors *versus* LMS/siRNA Vc cell tumors. The box graph depicts median ± S.D., and *error bars* show the minimum and maximum range of mitotic figures per 10 400× fields ($n = 15$). *, $p < 0.01$.

A decrease or functional loss through mutation in MED12 down-regulates β-catenin-mediated signaling, which is a major upstream transducer of versican expression (48). The relationship between MED12 mutation and a down-regulation in versican expression could potentially explain phenotypic differences between leiomyoma and LMS, benign *versus* metastatic tumors, but will require further study.

LMS tumors are characterized phenotypically as having less differentiated, highly synthetic, and highly proliferative smooth muscle cells with large atypically elongated nuclei, and multinucleated cells are not uncommon (49). We found that LMS cells and tumors were highly proliferative and migratory and produced an abundance of versican. Although features of atypia, cellularity, necrosis, and size correlate to some extent with malignancy, mitotic activity historically has been used as the most reliable parameter (49–51). Our findings that LMS tumor growth, tumor core necrosis, and mitotic index are dramatically reduced by decreasing the synthesis of versican further confirm the importance of the ECM in regulating cancer phenotype. LMS tumors that have a mitotic index (mitotic figures per 10 high power fields) of greater than 10 together with diffuse cytologic atypia and tumor cell necrosis highly correlate with metastases (52–54). In the present study, we observed a mitotic index of greater than 30 for the control LMS tumors along with high versican and hyaluronan levels and cytologic atypia. The LMS/siRNA Vc tumors in contrast had a mitotic index of less than 10 along with less cytologic atypia, no necrosis, and low levels of versican and hyaluronan.

In addition, we found that LMS cell adhesion could be increased or decreased through the modulation of versican levels. Yamagata and Kimata (55) demonstrated that reducing versican levels increased osteosarcoma cell adhesion, whereas in contrast increased expression of versican was correlated with low adhesion levels and metastatic spread of cancer cells (55, 56). The same was recently demonstrated by Bu and Yang (57) with the modulation of versican in malignant melanoma. In that study, the researchers showed that down-regulation of versican was directly correlated with decreased migration of the melanoma tumor cells. Moreover, other studies have shown that silencing of versican promotes cell adhesion to type I collagen, laminin, and fibronectin, indicating that versican plays proliferative, antiadhesive, and promigratory roles in melanoma (58). Nonetheless, the precise mechanism of the reciprocal relationship of versican with cell adhesion has not been established, but here we demonstrate that the adhesiveness of LMS cells can be modulated with the reduction or the addition of versican along with the pericellular coat thickness.

Recent studies indicate that versican may play additional roles in promoting the metastatic potential of certain cancers. For example, Kim *et al.* (13) showed that knocking down versican using shRNA significantly reduced the number of metastasized nodules in lungs and liver and the incidence of metastases when versican-depleted Lewis lung carcinoma cells were injected into tail veins of wild type mice. This and other studies (17, 59, 60) have demonstrated that versican secreted by tumors can induce macrophages to produce inflammatory cytokines that promote tumor growth and metastasis. Intriguingly, highly metastatic Lewis lung carcinoma cells express highly sulfated chondroitin sulfate such as chondroitin 4,6-sulfate (CS-E), and pretreatment of the cells with chondroitin ABC lyase or with blocking antibodies against chondroitin 4,6-sulfate significantly reduces lung metastases when the pretreated cells are injected into the tail veins of syngeneic mice (61). In the case of LMS, it may be that the expression of versican isoforms with abundant chondroitin sulfate chains (*e.g.* V0 and V1) by the LMS cells leads to a GAG-dependent localization and activation of cytokines, growth factors, and metalloproteinases (62, 63) that promote a proliferative and metastatic microenvironment.

Relationship of Hyaluronan and Versican in LMS Tumors and Tumor Cell Phenotype—Our finding of reduced levels of hyaluronan and mRNAs for HAS2 and HAS3 accompanying reduced levels of versican in LMS tumor cells suggests that these molecules, through a yet to be defined mechanism, may be co-regulated. Heightened levels of both hyaluronan and versican in tumor progression have been reported previously (45, 46, 64). It has also been reported that in many cancers the level of hyaluronan is considered to be a reliable prognostic indicator of malignant progression (65). Reduced levels of hyaluronan lead to significantly greater binding avidity of ovarian tumor cells to underlying mesothelium (53), whereas high levels of hyaluronan are correlated with increased migration and the ability of the cancer cells to traverse the ECM. Data from the overexpression of HAS1–3 or perturbation of hyaluronan production in several cancer cell lines have suggested that the accumulation of hyaluronan stimulates growth, survival, invasion, and metastasis of cancer cells (66–68). Thus, it is likely that both hyaluronan and versican participate in the formation of a permissive microenvironment around the LMS tumor cells to promote their proliferation (42, 69). It is interesting to note that our data show that a maximal proliferative response is achieved when the two molecules are added together, suggesting that a versican-hyaluronan complex may be optimal for the proliferative response of the LMS cells. The idea that versican and hyaluronan act synergistically and are co-regulated is underscored by our findings that the volume of the pericellular matrix, which consists primarily of hyaluronan (40), could be modulated by altering versican levels: knocking down versican reduced the pericellular volume, which was restored by exposure of the cells to purified versican. Moreover, we also determined that versican maintained or prevented the degradation of internalized hyaluronan. Ricciardelli *et al.* (70) showed that both versican and hyaluronan promoted malignant prostate epithelial cell migration, but predigestion with hyaluronidase (but not chondroitinase) reversed the increase in migration. In contrast to metastatic, rapidly proliferating LMS tumors, Mitropoulou *et al.* (71) observed that benign leiomyomas accumulated a lower amount of hyaluronan compared with normal, adjacent myometrium. In that study, the low amount of hyaluronan observed in leiomyomas was related to the low rate of growth and the benign nature of the tumor. In addition to a role for hyaluronan, our data suggest an additive role for versican in matrix-mediated tumor phenotypes.

Macromolecules such as versican and hyaluronan may influence the observed phenotype and facilitate tumorigenesis through cell surface signaling, *e.g.* versican through EGF receptor and integrin domains (72, 73) and hyaluronan through cell

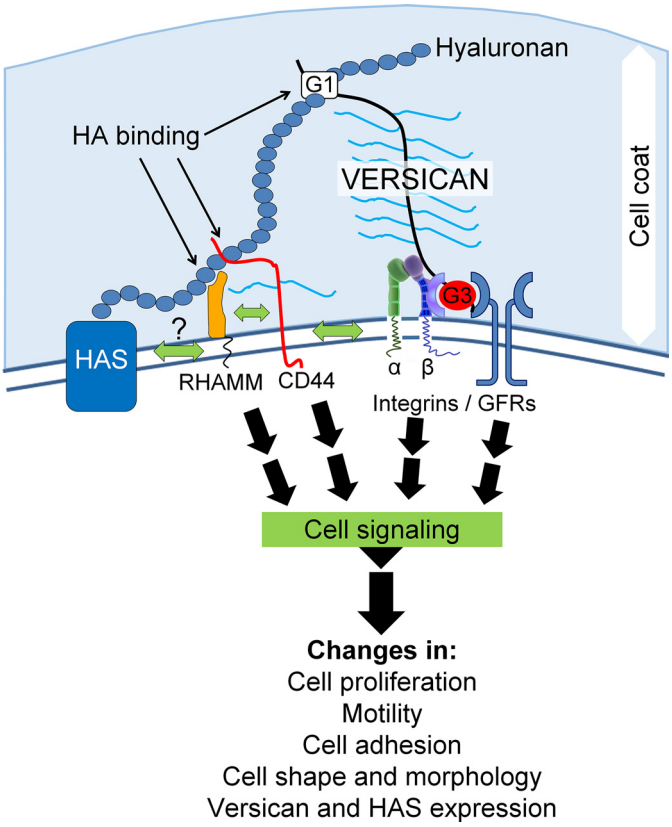

FIGURE 8. **Schematic diagram that details the described interplay of versican and hyaluronan in LMS tumorigenesis.** *RHAMM*, receptor for hyaluronan-mediated motility; *GFRs*, growth factor receptors; *HA*, hyaluronan.

surface hyaluronan-binding receptors CD44 and receptor for hyaluronan-mediated motility (74). This hypothesis is supported by recent studies that show that an siRNA-mediated down-regulation of versican leads to a corresponding reduction in CD44 (75), whereas an up-regulation of versican leads to a corresponding increase in CD44, matrix metalloproteinase-9, and receptor for hyaluronan-mediated motility (63). Moreover, overexpression of the G3 domain of versican in astrocytoma cells is associated with the development of larger tumors (72). This effect is attributed to modulation of cell signaling through the EGF receptor via versican G3 interactions. One hypothesis for the increased versican expression in a multitude of cancers, including our study, is that the interaction of hyaluronan with its receptor CD44 increases versican expression. CD44 has been shown to regulate cell migration in human colon cancer cells via Lyn kinase and AKT phosphorylation (76), and AKT phosphorylation is tied to GSK-3β/β-catenin activation (48). This is particularly significant as versican expression is in large part driven by the AKT/GSK-3β/β-catenin pathway (48). The activation of the CD44/AKT signaling axis by pericellular hyaluronan could explain the increased expression of versican observed in many cancer types, including the LMS tumors we examined. This hypothesis is supported by recent work by Kastner *et al.* (77) where treatment of mesangial cells with exogenous hyaluronan increased versican expression levels 3-fold. Thus, hyaluronan and versican may regulate one another in LMS with hyaluronan stimulating versican expression and versican levels modulating hyaluronan expression.

Taken together, our results describe the interplay of versican and hyaluronan in the control of LMS phenotype. For example, when versican was depleted, LMS proliferation, migration, and DNA replication were significantly reduced. Furthermore, the changes in versican expression changed both the expression of hyaluronan-synthesizing enzymes and the production of hyaluronan, which is required for cell division (78). Versican was also shown to be critical for preserving hyaluronan accumulation possibly by preventing its degradation. A role for versican in LMS tumors is diagrammatically depicted in Fig. 8. A reduction of versican shown in our study could impact signaling pathways by altering integrin β1 and/or growth factor receptor interactions necessary for proliferation and migration via the G3 domain of versican (7). Also, versican could influence CD44 and or receptor for hyaluronan-mediated motility signaling either directly or through effects on binding to hyaluronan. Nevertheless, changes in cell-to-matrix interactions of LMS cells mediated by versican and hyaluronan expression levels along with subsequent downstream signaling events suggest key roles for these molecules in the cancer biology of LMS and the focus of future studies.

In conclusion, we determined that the depletion of versican in LMS tumor cells by siRNA inhibits proliferation, migration, and hyaluronan expression *in vitro* and tumorigenic activity *in vivo*. These effects implicate this ECM proteoglycan as a potential point of control for treatment of LMS and other tumor types that express high levels of versican.

Acknowledgments—We thank Dr. Stephen Evanko, Dr. Michael Kinsella, and Dr. Robert Vernon for helpful discussions; Dr. Elizabeth Whalen, Kathleen Braun, and Christina Chan for technical assistance; and Dr. Virginia Green for careful editing and preparation of the manuscript.

REFERENCES

1. Major, F. J., Blessing, J. A., Silverberg, S. G., Morrow, C. P., Creasman, W. T., Currie, J. L., Yordan, E., and Brady, M. F. (1993) Prognostic factors in early-stage uterine sarcoma. A Gynecologic Oncology Group study. *Cancer* **71,** 1702–1709
2. Moinfar, F., Azodi, M., and Tavassoli, F. A. (2007) Uterine sarcomas. *Pathology* **39,** 55–71
3. Zako, M., Shinomura, T., Ujita, M., Ito, K., and Kimata, K. (1995) Expression of PG-M (V3), an alternatively spliced form of PG-M without a chondroitin sulfate attachment region in mouse and human tissues. *J. Biol. Chem.* **270,** 3914–3918
4. Wight, T. N., Kinsella, M. G., Evanko, S. P., Potter-Perigo, S., and Merrilees, M. J. (2014) Versican and the regulation of cell phenotype in disease. *Biochim. Biophys. Acta* **1840,** 2441–2451
5. Lemire, J. M., Braun, K. R., Maurel, P., Kaplan, E. D., Schwartz, S. M., and Wight, T. N. (1999) Versican/PG-M isoforms in vascular smooth muscle cells. *Arterioscler. Thromb. Vasc. Biol.* **19,** 1630–1639
6. Du, W. W., Yang, W., and Yee, A. J. (2013) Roles of versican in cancer biology—tumorigenesis, progression and metastasis. *Histol. Histopathol.* **28,** 701–713
7. Wu, Y. J., La Pierre, D. P., Wu, J., Yee, A. J., and Yang, B. B. (2005) The interaction of versican with its binding partners. *Cell Res.* **15,** 483–494
8. Bode-Lesniewska, B., Dours-Zimmermann, M. T., Odermatt, B. F., Briner, J., Heitz, P. U., and Zimmermann, D. R. (1996) Distribution of the large aggregating proteoglycan versican in adult human tissues. *J. Histochem. Cytochem.* **44,** 303–312
9. Theocharis, A. D., Skandalis, S. S., Tzanakakis, G. N., and Karamanos,

N. K. (2010) Proteoglycans in health and disease: novel roles for proteoglycans in malignancy and their pharmacological targeting. *FEBS J.* **277,** 3904–3923
10. Wight, T. N., Kang, I., and Merrilees, M. J. (2014) Versican and the control of inflammation. *Matrix Biol.* **35,** 152–161
11. Ricciardelli, C., Sakko, A. J., Ween, M. P., Russell, D. L., and Horsfall, D. J. (2009) The biological role and regulation of versican levels in cancer. *Cancer Metastasis Rev.* **28,** 233–245
12. Sakko, A. J., Ricciardelli, C., Mayne, K., Suwiwat, S., LeBaron, R. G., Marshall, V. R., Tilley, W. D., and Horsfall, D. J. (2003) Modulation of prostate cancer cell attachment to matrix by versican. *Cancer Res.* **63,** 4786–4791
13. Kim, S., Takahashi, H., Lin, W. W., Descargues, P., Grivennikov, S., Kim, Y., Luo, J. L., and Karin, M. (2009) Carcinoma-produced factors activate myeloid cells through TLR2 to stimulate metastasis. *Nature* **457,** 102–106
14. Labropoulou, V. T., Theocharis, A. D., Ravazoula, P., Perimenis, P., Hjerpe, A., Karamanos, N. K., and Kalofonos, H. P. (2006) Versican but not decorin accumulation is related to metastatic potential and neovascularization in testicular germ cell tumours. *Histopathology* **49,** 582–593
15. Nikitovic, D., Zafiropoulos, A., Katonis, P., Tsatsakis, A., Theocharis, A. D., Karamanos, N. K., and Tzanakakis, G. N. (2006) Transforming growth factor-β as a key molecule triggering the expression of versican isoforms v0 and v1, hyaluronan synthase-2 and synthesis of hyaluronan in malignant osteosarcoma cells. *IUBMB Life* **58,** 47–53
16. Gao, D., Vahdat, L. T., Wong, S., Chang, J. C., and Mittal, V. (2012) Microenvironmental regulation of epithelial-mesenchymal transitions in cancer. *Cancer Res.* **72,** 4883–4889
17. Said, N., Sanchez-Carbayo, M., Smith, S. C., and Theodorescu, D. (2012) RhoGDI2 suppresses lung metastasis in mice by reducing tumor versican expression and macrophage infiltration. *J. Clin. Investig.* **122,** 1503–1518
18. Arslan, A. A., Gold, L. I., Mittal, K., Suen, T. C., Belitskaya-Levy, I., Tang, M. S., and Toniolo, P. (2005) Gene expression studies provide clues to the pathogenesis of uterine leiomyoma: new evidence and a systematic review. *Hum. Reprod.* **20,** 852–863
19. Sobue, M., Takeuchi, J., Yoshida, K., Akao, S., Fukatsu, T., Nagasaka, T., and Nakashima, N. (1987) Isolation and characterization of proteoglycans from human nonepithelial tumors. *Cancer Res.* **47,** 160–168
20. Cattaruzza, S., Schiappacassi, M., Kimata, K., Colombatti, A., and Perris, R. (2004) The globular domains of PG-M/versican modulate the proliferation-apoptosis equilibrium and invasive capabilities of tumor cells. *FASEB J.* **18,** 779–781
21. Fletcher, C., Unni, K., and Mertens, F. (eds) (2002) *World Health Organization Classification of Tumours. Pathology and Genetics of Tumours of Soft Tissue and Bone,* 3rd Ed., Vol. 4, pp. 130–134, IARC Press, Lyon, France
22. Guillou, L., Coindre, J. M., Bonichon, F., Nguyen, B. B., Terrier, P., Collin, F., Vilain, M. O., Mandard, A. M., Le Doussal, V., Leroux, A., Jacquemier, J., Duplay, H., Sastre-Garau, X., and Costa, J. (1997) Comparative study of the National Cancer Institute and French Federation of Cancer Centers Sarcoma Group grading systems in a population of 410 adult patients with soft tissue sarcoma. *J. Clin. Oncol.* **15,** 350–362
23. du Cros, D. L., LeBaron, R. G., and Couchman, J. R. (1995) Association of versican with dermal matrices and its potential role in hair follicle development and cycling. *J. Invest. Dermatol.* **105,** 426–431
24. Chomczynski, P. (1993) A reagent for the single-step simultaneous isolation of RNA, DNA and proteins from cell and tissue samples. *BioTechniques* **15,** 532–534, 536–537
25. Schönherr, E., Kinsella, M. G., and Wight, T. N. (1997) Genistein selectively inhibits platelet-derived growth factor stimulated versican biosynthesis in monkey arterial smooth muscle cells. *Arch. Biochem. Biophys.* **339,** 353–361
26. Beck, A. H., Lee, C. H., Witten, D. M., Gleason, B. C., Edris, B., Espinosa, I., Zhu, S., Li, R., Montgomery, K. D., Marinelli, R. J., Tibshirani, R., Hastie, T., Jablons, D. M., Rubin, B. P., Fletcher, C. D., West, R. B., and van de Rijn, M. (2010) Discovery of molecular subtypes in leiomyosarcoma through integrative molecular profiling. *Oncogene* **29,** 845–854
27. Perou, C. M., Sørlie, T., Eisen, M. B., van de Rijn, M., Jeffrey, S. S., Rees, C. A., Pollack, J. R., Ross, D. T., Johnsen, H., Akslen, L. A., Fluge, O., Pergamenschikov, A., Williams, C., Zhu, S. X., Lønning, P. E., Børresen-Dale, A. L., Brown, P. O., and Botstein, D. (2000) Molecular portraits of human breast tumours. *Nature* **406,** 747–752
28. Eskander, R. N., Randall, L. M., Sakai, T., Guo, Y., Hoang, B., and Zi, X. (2012) Flavokawain B, a novel, naturally occurring chalcone, exhibits robust apoptotic effects and induces G2/M arrest of a uterine leiomyosarcoma cell line. *J. Obstet. Gynaecol. Res.* **38,** 1086–1094
29. Yang, J., Eddy, J. A., Pan, Y., Hategan, A., Tabus, I., Wang, Y., Cogdell, D., Price, N. D., Pollock, R. E., Lazar, A. J., Hunt, K. K., Trent, J. C., and Zhang, W. (2010) Integrated proteomics and genomics analysis reveals a novel mesenchymal to epithelial reverting transition in leiomyosarcoma through regulation of slug. *Mol. Cell. Proteomics* **9,** 2405–2413
30. Gao, C. F., Xie, Q., Zhang, Y. W., Su, Y., Zhao, P., Cao, B., Furge, K., Sun, J., Rex, K., Osgood, T., Coxon, A., Burgess, T. L., and Vande Woude, G. F. (2009) Therapeutic potential of hepatocyte growth factor/scatter factor neutralizing antibodies: inhibition of tumor growth in both autocrine and paracrine hepatocyte growth factor/scatter factor:c-Met-driven models of leiomyosarcoma. *Mol. Cancer Ther.* **8,** 2803–2810
31. Horiuchi, A., Nikaido, T., Mitsushita, J., Toki, T., Konishi, I., and Fujii, S. (2000) Enhancement of antitumor effect of bleomycin by low-voltage *in vivo* electroporation: a study of human uterine leiomyosarcomas in nude mice. *Int. J. Cancer* **88,** 640–644
32. Myslinski, E., Amé, J. C., Krol, A., and Carbon, P. (2001) An unusually compact external promoter for RNA polymerase III transcription of the human H1RNA gene. *Nucleic Acids Res.* **29,** 2502–2509
33. Fogh, J., and Trempe, G. (1975) in *Human Tumor Cells in Vitro* (Fogh, J., ed) pp. 115–159, Plenum Press, New York
34. Schönherr, E., Järveläinen, H. T., Sandell, L. J., and Wight, T. N. (1991) Effects of platelet-derived growth factor and transforming growth factor-β1 on the synthesis of a large versican-like chondroitin sulfate proteoglycan by arterial smooth muscle cells. *J. Biol. Chem.* **266,** 17640–17647
35. Hascall, V. C., Calabro, A., Midura, R. J., and Yanagishita, M. (1994) Isolation and characterization of proteoglycans. *Methods Enzymol.* **230,** 390–417
36. Olin, K. L., Potter-Perigo, S., Barrett, P. H., Wight, T. N., and Chait, A. (1999) Lipoprotein lipase enhances the binding of native and oxidized low density lipoproteins to versican and biglycan synthesized by cultured arterial smooth muscle cells. *J. Biol. Chem.* **274,** 34629–34636
37. Yu, Q., and Toole, B. P. (1995) Biotinylated hyaluronan as a probe for detection of binding proteins in cells and tissues. *BioTechniques* **19,** 122–124, 126–129
38. Underhill, C. B., Nguyen, H. A., Shizari, M., and Culty, M. (1993) CD44 positive macrophages take up hyaluronan during lung development. *Dev. Biol.* **155,** 324–336
39. Wilkinson, T. S., Potter-Perigo, S., Tsoi, C., Altman, L. C., and Wight, T. N. (2004) Pro- and anti-inflammatory factors cooperate to control hyaluronan synthesis in lung fibroblasts. *Am. J. Respir. Cell Mol. Biol.* **31,** 92–99
40. Evanko, S. P., Johnson, P. Y., Braun, K. R., Underhill, C. B., Dudhia, J., and Wight, T. N. (2001) Platelet-derived growth factor stimulates the formation of versican-hyaluronan aggregates and pericellular matrix expansion in arterial smooth muscle cells. *Arch. Biochem. Biophys.* **394,** 29–38
41. Hyacinthe, M., Jaroszeski, M. J., Dang, V. V., Coppola, D., Karl, R. C., Gilbert, R. A., and Heller, R. (1999) Electrically enhanced drug delivery for the treatment of soft tissue sarcoma. *Cancer* **85,** 409–417
42. Evanko, S. P., Tammi, M. I., Tammi, R. H., and Wight, T. N. (2007) Hyaluronan-dependent pericellular matrix. *Adv. Drug Deliv. Rev.* **59,** 1351–1365
43. Cattaruzza, S., and Perris, R. (2005) Proteoglycan control of cell movement during wound healing and cancer spreading. *Matrix Biol.* **24,** 400–417
44. Kodama, J., Hasengaowa, Kusumoto, T., Seki, N., Matsuo, T., Nakamura, K., Hongo, A., and Hiramatsu, Y. (2007) Versican expression in human cervical cancer. *Eur. J. Cancer* **43,** 1460–1466
45. Skandalis, S. S., Theocharis, A. D., Papageorgakopoulou, N., Vynios, D. H., and Theocharis, D. A. (2006) The increased accumulation of structurally modified versican and decorin is related with the progression of laryngeal cancer. *Biochimie* **88,** 1135–1143
46. Theocharis, A. D., Vynios, D. H., Papageorgakopoulou, N., Skandalis, S. S.,

and Theocharis, D. A. (2003) Altered content composition and structure of glycosaminoglycans and proteoglycans in gastric carcinoma. *Int. J. Biochem. Cell Biol.* **35,** 376–390
47. Mäkinen, N., Mehine, M., Tolvanen, J., Kaasinen, E., Li, Y., Lehtonen, H. J., Gentile, M., Yan, J., Enge, M., Taipale, M., Aavikko, M., Katainen, R., Virolainen, E., Böhling, T., Koski, T. A., Launonen, V., Sjöberg, J., Taipale, J., Vahteristo, P., and Aaltonen, L. A. (2011) MED12, the mediator complex subunit 12 gene, is mutated at high frequency in uterine leiomyomas. *Science* **334,** 252–255
48. Rahmani, M., Wong, B. W., Ang, L., Cheung, C. C., Carthy, J. M., Walinski, H., and McManus, B. M. (2006) Versican: signaling to transcriptional control pathways. *Can. J. Physiol. Pharmacol.* **84,** 77–92
49. Weiss, S., and Goldblum, J. (2001) *Enzinger and Weiss's Soft Tissue Tumors*, 4th Ed., pp. 695–748, Mosby, St. Louis, MO
50. Ranchod, M., and Kempson, R. L. (1977) Smooth muscle tumors of the gastrointestinal tract and retroperitoneum: a pathologic analysis of 100 cases. *Cancer* **39,** 255–262
51. Shmookler, B. M., and Lauer, D. H. (1983) Retroperitoneal leiomyosarcoma. A clinicopathologic analysis of 36 cases. *Am. J. Surg. Pathol.* **7,** 269–280
52. Perrone, T., and Dehner, L. P. (1988) Prognostically favorable "mitotically active" smooth-muscle tumors of the uterus. A clinicopathologic study of ten cases. *Am. J. Surg. Pathol.* **12,** 1–8
53. Jones, M. W., and Norris, H. J. (1995) Clinicopathologic study of 28 uterine leiomyosarcomas with metastasis. *Int. J. Gynecol. Pathol.* **14,** 243–249
54. Robboy, S. J., Bentley, R. C., Butnor, K., and Anderson, M. C. (2000) Pathology and pathophysiology of uterine smooth-muscle tumors. *Environ. Health Perspect.* **108,** Suppl. 5, 779–784
55. Yamagata, M., and Kimata, K. (1994) Repression of a malignant cell-substratum adhesion phenotype by inhibiting the production of the anti-adhesive proteoglycan, PG-M/versican. *J. Cell Sci.* **107,** 2581–2590
56. Yamagata, M., Saga, S., Kato, M., Bernfield, M., and Kimata, K. (1993) Selective distributions of proteoglycans and their ligands in pericellular matrix of cultured fibroblasts. Implications for their roles in cell-substratum adhesion. *J. Cell Sci.* **106,** 55–65
57. Bu, P., and Yang, P. (2014) MicroRNA-203 inhibits malignant melanoma cell migration by targeting versican. *Exp. Ther. Med.* **8,** 309–315
58. Hernández, D., Miquel-Serra, L., Docampo, M. J., Marco-Ramell, A., and Bassols, A. (2011) Role of versican V0/V1 and CD44 in the regulation of human melanoma cell behavior. *Int. J. Mol. Med.* **27,** 269–275
59. Li, D., Wang, X., Wu, J. L., Quan, W. Q., Ma, L., Yang, F., Wu, K. Y., and Wan, H. Y. (2013) Tumor-produced versican V1 enhances hCAP18/LL-37 expression in macrophages through activation of TLR2 and vitamin D3 signaling to promote ovarian cancer progression *in vitro*. *PLoS One* **8,** e56616
60. Bögels, M., Braster, R., Nijland, P. G., Gül, N., van de Luijtgaarden, W., Fijneman, R. J., Meijer, G. A., Jimenez, C. R., Beelen, R. H., and van Egmond, M. (2012) Carcinoma origin dictates differential skewing of monocyte function. *Oncoimmunology* **1,** 798–809
61. Li, F., Ten Dam, G. B., Murugan, S., Yamada, S., Hashiguchi, T., Mizumoto, S., Oguri, K., Okayama, M., van Kuppevelt, T. H., and Sugahara, K. (2008) Involvement of highly sulfated chondroitin sulfate in the metastasis of the Lewis lung carcinoma cells. *J. Biol. Chem.* **283,** 34294–34304
62. Ra, H. J., Harju-Baker, S., Zhang, F., Linhardt, R. J., Wilson, C. L., and Parks, W. C. (2009) Control of promatrilysin (MMP7) activation and substrate-specific activity by sulfated glycosaminoglycans. *J. Biol. Chem.* **284,** 27924–27932
63. Yeung, T. L., Leung, C. S., Wong, K. K., Samimi, G., Thompson, M. S., Liu, J., Zaid, T. M., Ghosh, S., Birrer, M. J., and Mok, S. C. (2013) TGF-β modulates ovarian cancer invasion by upregulating CAF-derived versican in the tumor microenvironment. *Cancer Res.* **73,** 5016–5028
64. Koyama, H., Hibi, T., Isogai, Z., Yoneda, M., Fujimori, M., Amano, J., Kawakubo, M., Kannagi, R., Kimata, K., Taniguchi, S., and Itano, N. (2007) Hyperproduction of hyaluronan in neu-induced mammary tumor accelerates angiogenesis through stromal cell recruitment: possible involvement of versican/PG-M. *Am. J. Pathol.* **170,** 1086–1099
65. Toole, B. P. (2004) Hyaluronan: from extracellular glue to pericellular cue. *Nat. Rev. Cancer* **4,** 528–539
66. Kosaki, R., Watanabe, K., and Yamaguchi, Y. (1999) Overproduction of hyaluronan by expression of the hyaluronan synthase Has2 enhances anchorage-independent growth and tumorigenicity. *Cancer Res.* **59,** 1141–1145
67. Li, Y., and Heldin, P. (2001) Hyaluronan production increases the malignant properties of mesothelioma cells. *Br. J. Cancer* **85,** 600–607
68. Liu, N., Gao, F., Han, Z., Xu, X., Underhill, C. B., and Zhang, L. (2001) Hyaluronan synthase 3 overexpression promotes the growth of TSU prostate cancer cells. *Cancer Res.* **61,** 5207–5214
69. Tofuku, K., Yokouchi, M., Murayama, T., Minami, S., and Komiya, S. (2006) HAS3-related hyaluronan enhances biological activities necessary for metastasis of osteosarcoma cells. *Int. J. Oncol.* **29,** 175–183
70. Ricciardelli, C., Russell, D. L., Ween, M. P., Mayne, K., Suwiwat, S., Byers, S., Marshall, V. R., Tilley, W. D., and Horsfall, D. J. (2007) Formation of hyaluronan- and versican-rich pericellular matrix by prostate cancer cells promotes cell motility. *J. Biol. Chem.* **282,** 10814–10825
71. Mitropoulou, T. N., Theocharis, A. D., Stagiannis, K. D., and Karamanos, N. K. (2001) Identification, quantification and fine structural characterization of glycosaminoglycans from uterine leiomyoma and normal myometrium. *Biochimie* **83,** 529–536
72. Zheng, P. S., Wen, J., Ang, L. C., Sheng, W., Viloria-Petit, A., Wang, Y., Wu, Y., Kerbel, R. S., and Yang, B. B. (2004) Versican/PG-M G3 domain promotes tumor growth and angiogenesis. *FASEB J.* **18,** 754–756
73. Sheng, W., Wang, G., Wang, Y., Liang, J., Wen, J., Zheng, P. S., Wu, Y., Lee, V., Slingerland, J., Dumont, D., and Yang, B. B. (2005) The roles of versican V1 and V2 isoforms in cell proliferation and apoptosis. *Mol. Biol. Cell* **16,** 1330–1340
74. Hamilton, S. R., Fard, S. F., Paiwand, F. F., Tolg, C., Veiseh, M., Wang, C., McCarthy, J. B., Bissell, M. J., Koropatnick, J., and Turley, E. A. (2007) The hyaluronan receptors CD44 and Rhamm (CD168) form complexes with ERK1,2 that sustain high basal motility in breast cancer cells. *J. Biol. Chem.* **282,** 16667–16680
75. Havre, P. A., Dang, L. H., Ohnuma, K., Iwata, S., Morimoto, C., and Dang, N. H. (2013) CD26 expression on T-anaplastic large cell lymphoma (ALCL) line Karpas 299 is associated with increased expression of versican and MT1-MMP and enhanced adhesion. *BMC Cancer* **13,** 517
76. Subramaniam, V., Vincent, I. R., Gardner, H., Chan, E., Dhamko, H., and Jothy, S. (2007) CD44 regulates cell migration in human colon cancer cells via Lyn kinase and AKT phosphorylation. *Exp. Mol. Pathol.* **83,** 207–215
77. Kastner, S., Thomas, G. J., Jenkins, R. H., Davies, M., and Steadman, R. (2007) Hyaluronan induces the selective accumulation of matrix- and cell-associated proteoglycans by mesangial cells. *Am. J. Pathol.* **171,** 1811–1821
78. Evanko, S. P., Angello, J. C., and Wight, T. N. (1999) Formation of hyaluronan- and versican-rich pericellular matrix is required for proliferation and migration of vascular smooth muscle cells. *Arterioscler. Thromb. Vasc. Biol.* **19,** 1004–1013
79. Lemire, J. M., Chan, C. K., Bressler, S., Miller, J., LeBaron, R. G., and Wight, T. N. (2007) Interleukin-1β selectively decreases the synthesis of versican by arterial smooth muscle cells. *J. Cell. Biochem.* **101,** 753–766